PROCEEDINGS OF THE ROYAL SOCIETY B

Proc. R. Soc. B (2005) **272**, 725–732
doi:10.1098/rspb.2004.3007
Published online 7 April 2005

Flexibility of spatial averaging in visual perception

Tania Lombrozo[1,2,*], Jeff Judson[1] and Donald I. A. MacLeod[1]

[1]*Department of Psychology, University of California at San Diego, La Jolla, CA 92093-0109, USA*
[2]*Department of Psychology, Harvard University, 33 Kirkland Street, Cambridge, MA 02138, USA*

The classical receptive field (RF) concept—the idea that a visual neuron responds to fixed parts and properties of a stimulus—has been challenged by a series of recent physiological results. Here, we extend these findings to human vision, demonstrating that the extent of spatial averaging in contrast perception is also flexible, depending strongly on stimulus contrast and uniformity. At low contrast, spatial averaging is greatest (about 11 min of arc) within uniform regions such as edges, as expected if the relevant neurons have orientation-selective RFs. At high contrast, spatial averaging is minimal. These results can be understood if the visual system is balancing a trade-off between noise reduction, which favours large areas of averaging, and detail preservation, which favours minimal averaging. Two distinct populations of neurons with hard-wired RFs could account for our results, as could the more intriguing possibility of dynamic, contrast-dependent RFs.

Keywords: spatial integration; contrast perception; anisotropy

1. INTRODUCTION

From the moment photons hit the retina, the visual system engages noise-reducing mechanisms to reconstruct a more faithful representation of stimuli in the environment. One such noise-reducing mechanism is spatial integration, which occurs when the visual system averages over a spatially extended region, such as an ellipse corresponding to some part of the visual field. By integrating over small areas of the visual field in this way, the visual system increases the extent to which photon and neural noise can be averaged out, and the signal corresponding to the stimulus more reliably transmitted. However, spatial integration has an associated cost, as averaging entails that detail contained within the averaged region will be lost. The situation is analogous to increasing the pixel size of a digital image—while some noise may be eliminated, the resolution will deteriorate.

In many situations the visual system faces a trade-off: noise reduction calls for larger regions of integration, but detail preservation requires smaller regions. The optimal compromise will depend on the stimulus being viewed. In particular, the signal-to-noise ratio (SNR) of the stimulus may be critical: the lower the signal level, the greater the need for noise-reducing mechanisms such as spatial integration. However, there are also situations in which this trade-off does not arise; namely, when the region over which spatial integration occurs is uniform. In this case, integration reduces noise without a cost in resolution, because there is no detail to be lost. SNR and local stimulus uniformity are therefore two of the properties relevant to spatial integration. In this paper, we examine how flexibly the human visual system handles the trade-off between detail preservation and noise reduction by measuring the extent of spatial integration in high- and low-noise contexts, and for both uniform and variable stimulus regions.

* Author for correspondence (lombrozo@wjh.harvard.edu).

To obtain estimates for the extent of spatial integration, we measure thresholds for the detection of non-uniformity in grating contrast (see figure 1 for sample stimuli). Measuring thresholds for the detection of subtle contrast modulations can yield estimates for the extent of spatial integration if detecting non-uniformities in contrast requires a certain grain of resolution. Specifically, to detect a contrast modulation, low- and high-contrast regions must be compared. However, if low- and high-contrast regions alternate with a sufficiently high spatial frequency, they will occur within the same window of integration, and the contrast modulation will fail to be detected. We can consequently estimate the extent of integration by observing how thresholds for detection of a contrast modulation are elevated as the spatial frequency of the modulation increases.

We use low and high contrast as high- and low-noise contexts, respectively. To detect an effect of uniformity, we employ stimuli with non-uniformities along otherwise uniform areas (grating bars), as well as across variable stimulus regions (grating bar contours). If greater integration occurs within uniform regions, then we would expect decreased sensitivity to non-uniformities within the uniform regions of the stimulus compared with variable regions. We find that this expected behaviour occurs only when contrast is low. At high contrast, when noise considerations presumably become less critical, spatial integration is minimal.

(a) *Previous work on spatial integration*

Both physiological and psychophysical tools have been previously employed to measure the extent of spatial integration at various stages of visual processing. Classically, the receptive field (RF) has been viewed as a hard-wired weighting function determining, in the spatial domain, the dimensions and location of the stimulus processed by that neuron. Hubel & Wiesel (1968) found elongated RFs in early cortical areas. When applied to correspondingly oriented image contours, such elongated

Received 6 September 2004
Accepted 8 November 2004

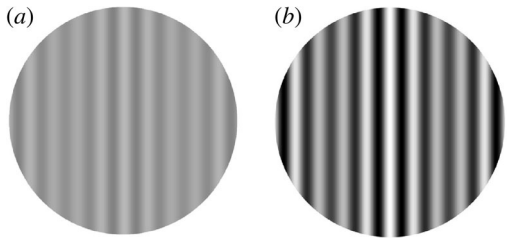

Figure 1. Examples of gratings used as stimuli, here illustrating parallel modulation. (*a*) Low-contrast stimulus (shown at higher contrast than in the experiment). (*b*) High-contrast stimulus.

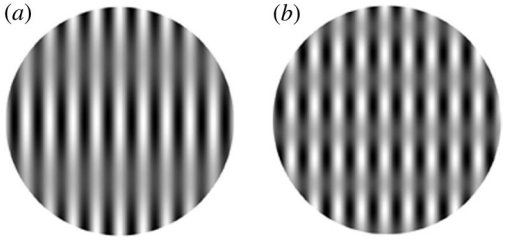

Figure 2. Examples of gratings used as stimuli, here illustrating orthogonal modulation. (*a*) Low modulation frequency stimulus. (*b*) High modulation frequency stimulus.

RFs yield anisotropic (i.e. non-circular) integration within uniform stimulus regions, thereby reducing noise while preserving resolution.

In psychophysics, studies have focused on determining the greatest regions over which visual information is spatially integrated. Jamar & Koenderink (1983) found that the ability to detect contrast differences in a grating increased with increasing number of grating cycles. Similarly, Legge & Foley (1980, 1981) found that grating contrast thresholds decreased as the number of cycles in a grating was increased. This could be accounted for by RFs with multiple excitatory and inhibitory regions, if the integration occurs at the level of individual neurons. Indeed, work by Sachs *et al.* (1971) and Kulikowski & King-Smith (1973) suggests the presence of RFs with weighting functions containing as many as eight or nine inhibitory and excitatory lobes. Alternatively, the increase in sensitivity over greater grating cycles could be due at least in part to probability summation (Robson & Graham 1981; Graham & Robson 1987): detectability may improve with increasing test pattern size not because individual neurons integrate over extended RFs, but because the multiple neurons stimulated by a large pattern each have a chance of detecting it.

To estimate the spatial extent of individual contrast-detecting units, Mostafavi & Sakrison (1976) and Jamar *et al.* (1982) used a modulation detection task. Jamar *et al.* (1982) measured sensitivity to amplitude modulation of sinusoidal luminance gratings, like those illustrated in figure 1, as well as to frequency modulation of sinusoidal luminance gratings. Their data suggest that, under the conditions tested, the spatial extent of contrast-detecting units does not exceed one cycle of the grating. Jamar *et al.* (1982), and Cropper (1998) more extensively, also examined how the contrast of the underlying grating (the carrier) influenced detection of a contrast modulation over that grating. Both studies found that increasing the carrier contrast elevates threshold contrast differences under some conditions, but no significant qualitative differences in modulation detection with increasing modulation frequency resulted from a change in the underlying carrier contrast.

The reviewed experiments have not provided evidence that the extent of spatial integration varies qualitatively with contextual properties such as contrast, and therefore SNR. Moreover, most studies have been restricted to examining integration across, rather than within, uniform bars of a grating stimulus (but see Lin & Wilson 1996; Dakin & Mareschal 2000; Mussap 2001). Such integration requires that input be averaged across a stimulus contour, and hence has an associated cost. It is possible that integration within uniform stimulus regions, where integration has no cost, is more extensive. In the present study, we employ a modulation detection task similar to that used by Jamar *et al.* (1982) and Cropper (1998). By measuring detection thresholds for contrast modulation occurring both within and across uniform stimulus regions, we assess the visual system's sensitivity to stimulus uniformity as well as to contrast.

2. METHODS

(a) *Stimuli and experimental procedure*

A two-alternative forced-choice procedure was used to determine the modulation detection threshold of an amplitude-modulated sinusoidal luminance grating. In each trial, the participant was presented with two 150 ms intervals, one containing an unmodulated sinusoidal grating (the carrier) and the other an amplitude-modulated sinusoidal grating (the modulated carrier; as in figures 1 and 2). The participant was asked to determine whether the modulated stimulus fell in the first or second interval of the trial. The carrier waveform was given by

$$I_c(x) = L[1 + c\cos(2\pi f_c x)], \tag{2.1}$$

where L is the mean luminance of the grating, c is the carrier contrast, f_c is the spatial frequency of the carrier, and x and y are the vertical and horizontal coordinates, respectively. In all cases, two carrier contrasts were measured, a 0.5 or 'high-contrast' condition, and a 0.05 or 'low-contrast' condition. Most of our data were collected with an f_c value of 8.5 cycles deg^{-1}, but carrier frequencies of up to 40 cycles deg^{-1} were also tested.

For the modulated carrier stimuli, the modulation was either parallel or orthogonal to the carrier grating. These gratings were given by the following equations for parallel (I_p) and orthogonal (I_o) modulation:

$$I_p(x,y) = L[1 + (c + \Delta c\cos(2\pi f_m x))\cos(2\pi f_c x)], \tag{2.2}$$

$$I_o(x,y) = L[1 + (c + \Delta c\cos(2\pi f_m y))\cos(2\pi f_c x)], \tag{2.3}$$

where f_m is the spatial frequency of the amplitude modulation, Δc is the contrast modulation (the difference between the grating's maximum local contrast and its space-average contrast), and the remaining values are as before. Figure 1 illustrates parallel contrast modulation. Figure 2 illustrates orthogonal contrast modulation.

Each stimulus had an abrupt onset and offset. Between stimulus presentations, participants fixated a small black dot in the centre of the screen. The phases of both the carrier and

modulation waveforms were adjusted such that both would peak at the fixation point. We also ran a control experiment with random phase to ensure that phase did not significantly alter threshold values. Participants were asked to indicate by a button press which interval contained the modulated stimulus. Feedback on accuracy was provided in the form of a beep for incorrect responses. The modulation contrast (Δc) was then varied according to a QUEST adaptive search algorithm adapted from the Pelli–Brainard–Zhang psychophysics toolbox for PC (Pelli & Zhang 1991; Brainard 1997). The algorithm was set to converge to an accuracy of 82% correct detection.

The number of trials per data point varied from 100 to 400. Data points corresponding to each curve were collected in a single session with interleaved conditions. Trials for each condition were presented in randomly ordered blocks of 20, with each block preceded by a brief presentation of the modulated grating at maximal modulation contrast (Δc), to show the participant what to look for in the subsequent 20 trials.

(b) *Apparatus*

The stimuli were displayed on a Nanao FlexScan 6600 monochrome monitor. An internal mixer in this monitor allows its green and blue inputs to be used together for precise control of grey levels, essentially in the manner of Pelli & Zhang (1991), with the B input contributing the less significant bits. The monitor was calibrated using a United Detector Technology S370 photometer to create a linear look-up table with 4096 entries corresponding to distinct linearly spaced grey levels. Owing to software and hardware limitations, however, only 256 of these grey levels could be simultaneously displayed. To create an optimal 256 entry palette of greys for each stimulus presentation, we estimated the maximum contrast potentially needed for the desired stimulus. We then sampled the 4096 entry look-up table at equally spaced values that spanned only the required range of contrast values. Later experiments were conducted identically with the exception of a Cambridge Research VSG 15 bit video board. In this case, only the green input to the Nanao was used, and the output was linearized using the above photometer.

The stimuli were presented in a circular window with a diameter of 8 degrees of visual angle from a distance of 1.65 m. The resolution was approximately 60 pixels horizontally and vertically per degree of visual angle. The mean luminance, both during and between stimulus presentations, was about 74 cd m^{-2}.

(c) *Participants*

Six observers (including the first and second authors) participated in the experiment. T. L., M. W. and J. J. took part in all conditions, while I. F., I. M. and T. M. took part in the primary experimental condition and some control conditions. Both I. F. and J. J. were experienced observers, and most participants were naive to the purposes of the experiment. All observers had normal or corrected-to-normal vision.

3. RESULTS

(a) *Estimate of the extent of spatial integration*

The thresholds we obtained for the detection of non-uniformity in grating contrast can be used to estimate the extent of spatial integration in each condition. As the frequency of the contrast modulation increases, participants are required to detect increasingly fine-scale differences in contrast. Assuming a fixed window of integration for a given contrast and modulation orientation, we would expect a decrease in sensitivity once the differences in contrast occur within the window of integration, and are hence averaged out. Thus as modulation frequency increases, a decrease in sensitivity, i.e. increase in threshold, occurs when one cycle of modulation almost fills the window of integration.

Figure 3 illustrates the measured threshold values for all four conditions, along with a trend line indicating the average regression line for all observers. The data shown here were collected with a carrier spatial frequency of 8.5 cycles deg^{-1}. Conditions with a positive slope suggest that some integration is taking place, where the extent of integration is a function of the slope (we formalize this analysis in Appendix A). The only condition with a consistently positive slope was the low-contrast orthogonal condition: all participants had a slope significantly greater than zero ($p < 0.01$), with a mean of 0.248. A clear trend is shown by 5 cycles deg^{-1}, in which five and six participants were tested in the parallel and orthogonal cases, respectively. Additional data were obtained at up to 8 cycles deg^{-1} for fewer participants and reinforce this trend. In the low-contrast parallel condition, the average slope was only 0.019, and was not significantly different from zero for any participant ($p < 0.01$).

The slopes were more variable in the high-contrast cases, but hovered around zero. In the high-contrast orthogonal case, slopes ranged from -0.064 to 0.067, with an average of 0.004. For the high-contrast parallel condition, the average slope was -0.083, with a range of -0.121 to -0.054. Two observers' slopes in this condition did not differ significantly from zero ($p < 0.01$); the remaining three observers' slopes were slightly less than zero.

Thus the only condition with substantial integration was the low-contrast orthogonal case—the condition where the SNR was low and there was little cost to integration because of the region's uniformity. The analysis in Appendix A suggests that the extent of integration was on average about 11.0 min of arc, with individual observers ranging from 6.8 to 17.0 min of arc (see figure 4). In the high-contrast orthogonal condition, even those observers with statistically significant slopes yielded a much lower average integration estimate of 2.4 min of arc, with a range of 1.4–3.0 min.

These estimates assume that our task indeed reflects spatial integration and not detection of the sideband components of the stimuli or a distortion product. We explore and eliminate such alternative explanations for the data in Appendix B, where several control experiments are detailed.

(b) *Effects of contrast and uniformity*

Figure 3 also illustrates the dependence of modulation detection threshold on contrast. As expected from studies of masking (e.g. Legge & Foley 1980), in which the contrast necessary for detecting a target grating typically increases with the contrast of the mask, the threshold spatial variation in contrast increased with the contrast of

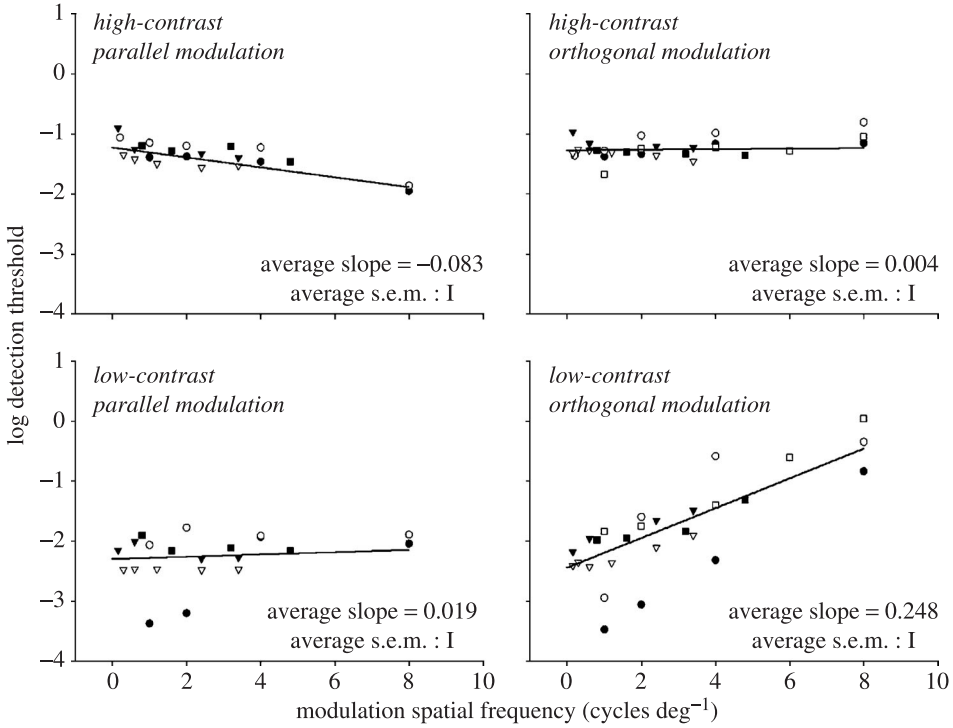

Figure 3. Data in the primary modulation detection task for six observers: T. M. (black circles), J. J. (white circles), M. W. (black triangles), T. L. (white triangles), I. F. (black squares) and I. M. (white squares). The *y*-axis represents log detection threshold, while the *x*-axis represents modulation spatial frequency in cycles deg^{-1}. 'High contrast' corresponds to a carrier contrast of 0.5 and 'low contrast' to a carrier contrast of 0.05. The carrier frequency for all conditions was 8.5 cycles deg^{-1}. The solid line corresponds to the average regression line for each set of data.

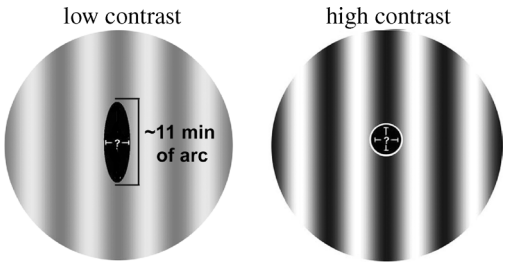

Figure 4. Estimated extent of parallel and orthogonal integration superimposed on a grating like those used as stimuli. The superimposed receptive field illustrates our estimate of 11.0 min of arc of integration along uniform stimulus bars at low contrast, and minimal integration in other conditions. The scale assumes an 8.5 cycles deg^{-1} carrier.

the carrier. We found that contrast also interacted with stimulus uniformity. When contrast modulation was parallel, the thresholds were almost constant as modulation frequency increased, whatever the contrast. Conversely, for orthogonal modulation, thresholds increased substantially with modulation frequency, but only at low contrast.

(c) *Interpretation of downward trends*

Although variation in the extent of spatial integration can account for the upward trend in the data in figure 3 for the low-contrast orthogonal condition, it cannot account for the slight downward trend seen in the high-contrast parallel condition. Two mechanisms could account for this trend. First, if the cortical neurons that respond well to high modulation frequencies have correspondingly high sampling densities, the consequent availability of more neural signals could lead to lower thresholds, through an averaging of the signals or through probability summation.

A second possibility is that the downward trend reflects the extent of a region governing contrast gain. Assuming that contrast gain is determined by a set region for a given carrier frequency and contrast, then when contrast modulation of the carrier is of a low enough frequency, entirely low- or high-contrast regions will fall within the region that determines the contrast gain. Contrast gain will compensate for the low-frequency modulation, resulting in a stimulus that is represented as globally uniform. However, when modulation is of a high enough frequency to yield both high- and low-contrast regions within the area that sets the gain, such local compensation will not occur. In this way, contrast-gain control might lead to higher detection thresholds for lower modulation frequencies. Such a sensitivity trend was clearly observed under all four conditions at lower modulation frequencies than those of figure 3.

4. DISCUSSION

We began by considering the role of spatial integration in noise reduction, and concluded that because it requires a loss in resolution, integration should be applied selectively. Indeed, we found that integration subtends about 11.0 min of arc at low contrast within uniform grating bars, but is minimal in the remaining conditions. This suggests that the extent of integration can change with stimulus context in a way that is sensitive to both SNR

(at least as determined by contrast) and to local stimulus structure, like uniformity.

Our estimates for the extent of spatial averaging are considerably smaller than those previously estimated with independent methods, including other psychophysical tasks (Legge & Foley 1980, 1981; Jamar & Koenderink 1985). We believe that this discrepancy is due to the specific demands of the task we employed. Small-scale non-uniformities in contrast will be best detected by the neurons with the smallest regions of integration, so our task determines a lower limit on integration. Simple grating-detection tasks can benefit from long-range integration and hence serve to identify the upper limit on the extent of integration.

While our data support the claim that contrast can influence the extent of spatial integration, our analysis suggests that other stimulus properties that influence SNR should have a similar effect. In a set of quite different experiments, Barlow *et al.* (1957, 1972) found evidence for a reduction in spatial integration with increasing luminance. Our results and Barlow's fit within a common framework: just as SNR increases with luminance when photon noise is limiting, it increases with contrast when fluctuations in the impulse counts of contrast-sensitive visual neurons are limiting. The influence of uniformity may likewise extend to a broader class of stimulus properties. We examined the difference between integration along a completely uniform grating bar, in which luminance and other properties like colour remain constant, with integration across a grating bar contour, in which luminance changes sinusoidally. An interesting question for future research is what kinds of stimulus non-uniformities, other than sinusoidal luminance changes, also induce minimal spatial integration.

Finally, it is worth considering the cortical physiological mechanisms that could account for our finding that spatial averaging depends on contrast. One possibility is that observers make use of a range of different, hard-wired RF sizes. Neurons with very small RFs might become important only at high contrast, where the SNR is favourable enough to render them reliable. Neurons with larger RFs may saturate at high-contrast levels, leaving the smaller RFs to perform the crucial detection.

Alternatively, RFs may actually change with contrast. This option is attractive given physiological work by Sceniak *et al.* (1999) that found a measurable change in RF size with contrast in primary visual cortex. The size of this effect may not be great enough to account for the data reported here. Nonetheless, the idea that RFs are dynamic and capable of being manipulated by stimulus properties has been suggested by a number of recent results (Levitt & Lund 1997; Ringach *et al.* 1997), presenting an effective challenge to the classical RF concept.

A third possibility is that this task involves two distinct processing stages. In the first stage, the large RFs typical of primary visual cortex attenuate the contrast modulation. But in the subsequent stages of processing an inverse filter might compensate for the previous neural stages' attenuation of high spatial frequencies, effectively 'undoing' the averaging originating at the first stage so as to reconstruct a more faithful representation of the original stimulus. The inverse filter need not be hard-wired, but could reflect an observer's ability to use the signals from the first stage in the way best suited to performance of the task. Such computations would preserve information in a noiseless system, but the amplification at high spatial frequencies would amplify noise along with the signal. This could discourage their application to low-contrast images, where the neural representation is contaminated by random variation in the firing rates of contrast-driven neurons (Kaplan & Shapley 1986; Lee *et al.* 1990).

Whatever its mechanistic basis, our finding that spatial integration varies with stimulus properties such as uniformity and contrast adds to a growing body of evidence, both physiological and psychophysical, that the functional organization of the visual system is adaptively sensitive to properties of stimulus and context.

We thank N. Graham, S. McKee, R. Shapley, T. Griffiths and M. Weisberg for helpful comments. This research was supported by NIH grant EY01711. A preliminary report of these findings was presented at the annual meeting of the Association for Research in Vision and Ophthalmology, May 2000.

APPENDIX A

Here, we explain how our quantitative estimates of the extent of spatial integration were calculated based on thresholds for the detection of contrast modulation, as illustrated in figure 3. We discuss the case of low carrier contrast with orthogonal modulation (equation (2.3)), since only that condition revealed substantial spatial integration. Along the vertical lines where carrier luminance peaks, the local luminance fluctuates about its average value by $L\Delta c\cos(2\pi f_{\mathrm{m}}y)$; the deviation from the space average luminance varies between $+L\Delta c$ at the y-value where local contrast is maximal and $-L\Delta c$ where it is minimal. A neuron with an RF centred on the point of maximum luminance averages the maximum luminance with nearby lesser luminances, with weights given by the vertical cross-section of the RF profile $s(y)$. Consequently, spatial integration along the bars will effectively reduce the amplitude of this excursion in luminance; the effective amplitude at the spatially integrated output becomes proportional to the integrated cross-product $s(y)\cos(2\pi f_{\mathrm{m}}y)$, and if $s(y)$ is even, this will be proportional to the cosine Fourier transform of $s(y)$. Here, for simplicity, we neglect spatial integration across the bars, as our results indicate that its range is restricted enough for the carrier profile to be approximately uniform across the RF.

The nearly straight-line relations indicated in figure 3 between the log of the threshold modulation Δc and modulation frequency imply exponential relations between sensitivity (the reciprocal of threshold) and modulation frequency. Denoting sensitivity by $S(f_{\mathrm{m}})$,

$$S(f_{\mathrm{m}}) = S_0\exp(-\alpha|2\pi f_{\mathrm{m}}|), \qquad \text{(A 1)}$$

where S_0 is the sensitivity approached as the modulation frequency approaches zero and where the value of α depends on the slope of the fitted line. Sensitivity is reduced by a factor $1/e$ at $f_{\mathrm{m}}=1/(2\pi\alpha)$ cycles deg^{-1}.

As a simple working hypothesis to relate these data to RF profiles, we assume that detection of modulation requires the same modulation in effective luminance, or in effective contrast, at all modulation frequencies f_{m}. The variation

of modulation sensitivity with f_m is then inversely proportional to the factor by which spatial filtering attenuates the modulation. Since the $1/e$ value of f_m is approximately 2 cycles deg^{-1} for the average of the observers shown, we have $\alpha = 5.5$ min of arc for our observers. The corresponding spatial RF profile $s(y)$ is

$$s(y) = S_0\alpha/(\alpha^2 + y^2). \quad \text{(A 2)}$$

This falls to half maximum height at $y = \pm\alpha$, or ± 5.5 min of arc. At half-height this translates to an integration range of about 11.0 min of arc. A similar analysis for those observers with a positive slope in the high-contrast orthogonal condition suggests an average integration range of about 2.4 min of arc. Since there is no consistent and measurable upward trend in the results for the other two conditions, the results suggest minimal spatial integration in those cases; an integration range as small as 1 min of arc would have been experimentally detectable.

APPENDIX B

We ran several control experiments to check the possibility that thresholds were influenced by independent detection of sideband Fourier components of the image, rather than by sensitivity to contrast modulation as such. The product of two sinusoidal functions can be decomposed into two Fourier components, or sidebands. The amplitude-modulated stimuli used in our experiment can consequently be expressed as the sum of the carrier frequency and two sideband components:

$$I_p = I_c + L[(\Delta c/2)\sin(\pi/2 - (2\pi)(f_c - f_m)x)] + L[(\Delta c/2)\sin(\pi/2 - (2\pi)(f_c + f_m)x)], \quad \text{(B 1)}$$

$$I_o = I_c + L[(\Delta c/2)\sin(\pi/2 - (2\pi)(f_c x - f_m y))] + L[(\Delta c/2)\sin(\pi/2 - (2\pi)(f_c x - f_m y))]. \quad \text{(B 2)}$$

In this section, we present data for control experiments relevant to the hypothesis that modulation detection thresholds are determined by independent detection of these sideband components. This hypothesis makes several predictions about how observers will perform on tasks related to amplitude modulation detection.

As Δc increases, each sideband increases in contrast as well. Specifically, each sideband will have a contrast equal to half of Δc. If modulation detection thresholds are governed by sideband detection, we would expect one of the sidebands to be detectable when its contrast is at most half of the contrast necessary for the amplitude modulation to be visible. We ran a simple detection experiment for the lower-frequency sideband corresponding to each amplitude modulation and carrier frequency. Because of the shape of the contrast-sensitivity function, we reasoned that the lower-frequency sideband would be more detectable. The method was varied from the principal experiment only in that each interval in the forced-choice task contained either the single sideband grating or a uniform field at a mean luminance equal to that of the grating. The values we obtained from this experiment are plotted in figure 5 for one participant. The actual sideband detection thresholds are not only much greater than the predicted values, they are greater than the amplitude modulation detection thresholds. The only exception to this is for the highest modulation data point for participant J. J., where the detection threshold is not significantly different from the predicted value. This strongly suggests that sideband detection does not determine the threshold values, at least not in the low-contrast condition.

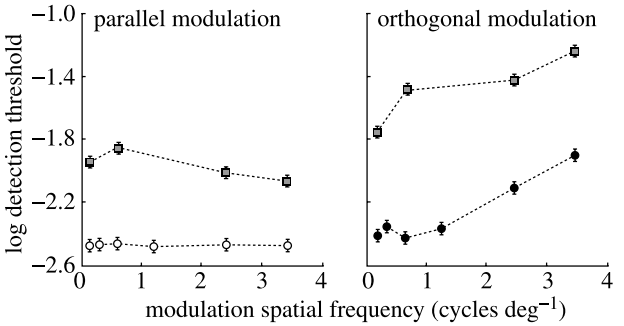

Figure 5. Sideband detection for low contrast: data from participant T. L. in the sideband-control experiment for the low-contrast carrier condition. White circles correspond to detection thresholds for parallel modulation, and black circles to thresholds for orthogonal modulation. The grey squares are the thresholds collected for detection of the lower-frequency sideband corresponding to each modulation direction and spatial frequency. The latter thresholds are higher, suggesting that sideband detection is not governing modulation detection thresholds at low contrast. Here again, carrier spatial frequency is 8.5 cycles deg^{-1}.

To assess the plausibility of independent sideband detection in the high-contrast case, we can examine the predicted behaviour of the curves as the modulation frequency increases. In the case where contrast varies orthogonally, the two sidebands have the same spatial frequency but differ in orientation. The sideband spatial frequency is always greater than the carrier frequency and increases with the modulation frequency, as does the deviation from vertical orientation. We measured the detection threshold for a range of spatial frequencies (8–14 cycles deg^{-1}) and orientations ($-25°$ to $25°$) for participant T. L. As expected, we found that sensitivity decreases as orientation deviates from vertical and as the spatial frequency increases. This suggests that the sidebands should become less detectable with increasing modulation frequency. Given this model, we would expect observers to become less sensitive to orthogonal modulation at high contrast as the spatial frequency of the modulation increases. As there was no significant upward trend in the high-contrast orthogonal case, however, it seems unlikely that thresholds are governed by sideband detection.

In the case where contrast modulation is parallel, the spatial frequencies of the sidebands are determined by the sum and difference of the carrier and modulation spatial frequencies. As the modulation frequency increases, the spatial frequency of the lower-frequency sideband decreases, thus rendering it more detectable. This suggests that the threshold values should decrease with increasing modulation frequency. Because this is consistent with the collected data, we ran a more rigorous test to examine the independent sideband detection hypothesis in the high-contrast condition with parallel modulation. We produced a single sideband, or 'beat,' stimulus by

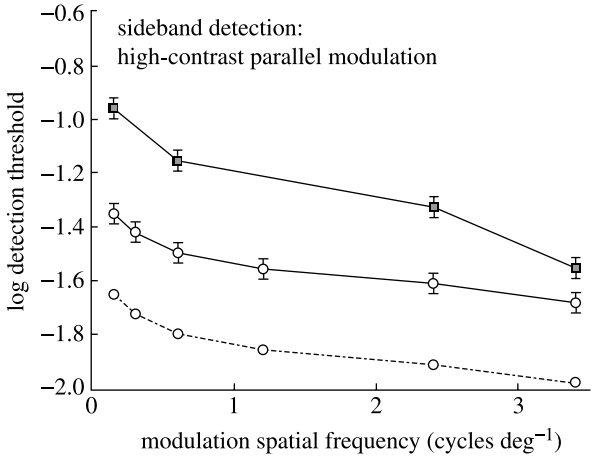

Figure 6. Data for participant T. L. in the sideband-control experiment for the high-contrast, 8.5 cycles deg^{-1} carrier condition with parallel modulation. The white circles along the solid line correspond to the thresholds measured for detection of modulation at high contrast and for parallel modulation. Based on these values, we calculated the predicted beat detection thresholds, shown here as white circles along a dotted line. The actual beat thresholds, shown as grey squares, were greater than the prediction, suggesting that sideband detection does not account for modulation detection in the high-contrast case with parallel modulation.

adding the carrier frequency to the lower-frequency sideband. The stimulus was given by

$$I_b = I_c + L[(\Delta c/2)\sin(\pi/2 - (2\pi)(f_c - f_m)x)]. \quad \text{(B 3)}$$

This produced an amplitude modulation as well as a minimal frequency modulation. The carrier contrast, at 0.5, was identical to the high-contrast case in the main experiment. Because each sideband received only half of the Δc as in the main experiment, we would expect the single sideband to require $\Delta c/2$ to become detectable. This would lead to a significantly lower detection threshold for the single sideband stimulus than the true amplitude modulation stimulus. Figure 6 shows the data obtained for the high-contrast case of parallel modulation, as well as the predictions for beat detection based on these data. The actual thresholds for the beat experiment, also shown, are in fact higher than those predicted, implying that sideband detection cannot account for the modulation detection thresholds in the main experiment.

Bodis-Wollner *et al.* (1973) found evidence to suggest that detection of an amplitude-modulated grating is governed by the detection threshold of the sideband components. However, Bodis-Wollner's stimuli differed from ours in introducing modulations at frequencies greater than half of the spatial frequency of the carrier. With a parallel modulation at half the spatial frequency of the carrier, the stimulus will appear to have alternating light and dark bars. When the modulation frequency exceeds this value, contrast changes occur within the uniform regions of a grating bar. Jamar *et al.* (1982) likewise found that thresholds for amplitude-modulated gratings could be predicted from the sideband components for these higher modulation frequencies, but not for the range of frequencies used in our experiments. Therefore, there is no real inconsistency between previous results and our finding that, for the conditions tested, sideband detection does not determine the thresholds for detecting the amplitude-modulated grating.

Another possibility is that a nonlinearity in visual processing introduces energy at the modulation frequency, and that participants are detecting this distortion product. Badcock & Derrington (1989) and Cropper (1998) tested this hypothesis in the conditions relevant to our experiment, and found no evidence for such a distortion product.

REFERENCES

Badcock, D. R. & Derrington, A. M. 1989 Detecting the displacement of spatial beats: no role for distortion products. *Vision Res.* **29**, 731–739.

Barlow, H. B. 1972 Dark and light adaptation: psychophysics. In *Handbook of sensory physiology*, vol. VII/4 (ed. D. Jameson & L. M. Hurvich), pp. 1–28, Berlin: Springer-Verlag.

Barlow, H. B., Fitzhugh, R. & Kuffler, S. W. 1957 Change of organization in the receptive fields of the cat's retina during dark adaptation. *J. Physiol.* **137**, 338–354.

Bodis-Wollner, I., Diamond, S. P., Orlofsky, A. & Levinson, J. 1973 Detection of spatial chages of the contrast of a grating pattern. *J. Opt. Soc. Am.* **63**, 1296.

Brainard, D. H. 1997 The psychophysics toolbox. *Spat. Vis.* **10**, 433–436.

Cropper, S. J. 1998 Detection of chromatic and luminance contrast modulation by the visual system. *J. Opt. Soc. Am. A* **15**, 1969–1986.

Dakin, S. C. & Mareschal, I. 2000 Sensitivity to contrast modulation depends on carrier spatial frequency and orientation. *Vision Res.* **40**, 311–329.

Graham, N. & Robson, J. G. 1987 Summation of very close spatial frequencies: the importance of spatial probability summation. *Vision Res.* **27**, 1997–2007.

Hubel, D. H. & Wiesel, T. N. 1968 Receptive fields and functional architecture of monkey striate cortex. *J. Physiol.* **195**, 215–243.

Jamar, J. H. T. & Koenderink, J. J. 1983 Sine-wave gratings: scale-invariance and spatial-integration at suprathreshold contrast. *Vision Res.* **23**, 805–810.

Jamar, J. H. T. & Koenderink, J. J. 1985 Contrast detection and detection of contrast modulation for noise gratings. *Vision Res.* **25**, 511–521.

Jamar, J. H. T., Campagne, J. C. & Koenderink, J. J. 1982 Detectability of amplitude and frequency-modulation of suprathreshold sine-wave gratings. *Vision Res.* **22**, 407–416.

Kaplan, E. & Shapley, R. M. 1986 The primate retina contains two types of ganglion cells, with high and low contrast sensitivity. *Proc. Natl Acad. Sci. USA* **83**, 2755–2757.

Kulikowski, J. J. & King-Smith, P. E. 1973 Spatial arrangement of line, edge, and grating detectors revealed by subthreshold summation. *Vision Res.* **13**, 1455–1478.

Lee, B. B., Pokorny, J., Smith, V. C., Martin, P. R. & Valberg, A. 1990 Luminance and chromatic modulation sensitivity of macaque ganglion cells and human observers. *J. Opt. Soc. Am. A* 7, 2223–2236.

Legge, G. E. & Foley, J. M. 1980 Contrast masking in human vision. *J. Opt. Soc. Am. A* **70**, 1458–1471.

Legge, G. E. & Foley, J. M. 1981 Contrast detection and near-threshold discrimination in human vision. *Vision Res.* **7**, 1041–1053.

Levitt, J. B. & Lund, J. S. 1997 Contrast dependence of contextual effects in primate visual cortex. *Nature* **387**, 73–76.

Lin, L. M. & Wilson, H. R. 1996 Fourier and non-Fourier pattern discrimination compared. *Vision Res.* **13**, 1907–1918.

Mostafavi, H. & Sakrison, D. J. 1976 Structure and properties of a single channel in the human visual system. *Vision Res.* **16**, 957–968.

Mussap, A. J. 2001 Orientation integration in detection and discrimination of contrast-modulated patterns. *Vision Res.* **41**, 295–311.

Pelli, D. G. & Zhang, L. 1991 Accurate control of contrast on microcomputer displays. *Vision Res.* **31**, 1337–1350.

Ringach, D. L., Hawken, M. J. & Shapley, R. 1997 Dynamics of orientation tuning in macaque primary visual cortex. *Nature* **387**, 281–284.

Robson, J. G. & Graham, N. 1981 Probability summation and regional variation in contrast sensitivity across the visual field. *Vision Res.* **21**, 409–418.

Sachs, M. B., Nachmias, J. & Robson, J. G. 1971 Spatial-frequency channels in human vision. *J. Opt. Soc. Am. A* **61**, 1176–1186.

Sceniak, M. P., Ringach, D. L., Hawken, M. J. & Shapley, R. 1999 Contrast's effect on spatial summation by macaque V1 neurons. *Nat. Neurosci.* **2**, 733–739.

As this paper exceeds the maximum length normally permitted, the authors have agreed to contribute to production costs.